

Floquet engineering a bosonic Josephson junction

Si-Cong Ji,¹ Thomas Schweigler,^{1,2} Mohammadamin Tajik,¹ Federica Cataldini,¹
 João Sabino,^{1,3,4} Frederik S. Møller,¹ Sebastian Erne,¹ and Jörg Schmiedmayer^{1,*}

¹Vienna Center for Quantum Science and Technology (VCQ), Atominstytut, TU Wien, Vienna, Austria

²JILA, University of Colorado, Boulder, Colorado, USA

³Instituto Superior Técnico, Universidade de Lisboa, Lisbon, Portugal

⁴Instituto de Telecomunicações, Physics of Information and Quantum Technologies Group, Lisbon, Portugal

(Dated: February 15, 2022)

We study Floquet engineering of the tunnel coupling between a pair of one-dimensional bosonic quasi-condensates in a tilted double-well potential. By modulating the energy difference between the two wells, we re-establish tunnel coupling and precisely control its amplitude and phase. This allows us to initiate coherence between two initially uncorrelated Bose gases and prepare different initial states in the emerging sine-Gordon Hamiltonian. We fully characterize the Floquet system and study the dependence of both equilibrium properties and relaxation on the modulation.

Introduction.—Periodic driving, i.e. Floquet engineering, offers a wide range of pathways to design effective Hamiltonians which are otherwise difficult to achieve or even unrealizable in static laboratory systems [1–3]. For ultracold atoms, Floquet engineering has been used in optical lattices to coherently control tunneling between sites [4–8], applied to generate large artificial gauge fields [9–11] and to simulate the quantum Hall effect [12–15]. Proposals for continuous systems range from implementing the Pokrovsky-Talapov model [16–18], used to describe the Commensurate-Incommensurate phase transition [19], to analogue simulators for pre-heating [20] and false-vacuum decay [21]. Experimental studies on continuous interacting many-body Floquet systems and their equilibration process are, however, limited. In this letter we present an experimental study of Floquet engineering tunneling and phase locking in a pair of continuous one-dimensional superfluids in a tilted double well (DW).

Experimental setup and Floquet engineering—Our experiment (Fig. 1) starts with a pair of tunnel-coupled one-dimensional (1D) Bose gases of ⁸⁷Rb atoms trapped in a DW potential created on an atom chip [22, 23] by radio-frequency (RF) dressing [24, 25]. For both wells, the trapping frequencies are $\omega_{\perp} = 2\pi \times 1.4$ kHz transversely and $\omega_z = 2\pi \times 10$ Hz longitudinally. We prepare the system (total atom number $N \approx 10^4$, peak density $\rho_0 \approx 50 \mu\text{m}^{-1}$) through evaporative cooling in a balanced DW potential. The initial temperature of the samples is $T_i \approx 37(5)$ nK as measured by the two-point density correlation function after 11.2 ms Time-of-Flight (ToF) [26]. In the longitudinal direction, the spatially resolved relative phase between the superfluids is extracted from matter-wave interference after 15.6 ms ToF. For the further analysis we use the central 50 μm (variation of density less than 15%). Expectation values are calculated by averaging over 30-60 experimental realizations.

The RF dressing allows precise control over the DW potential, determining the barrier height, i.e. the tunnel coupling J , and the potential energy difference ΔE between the two wells (Fig. 1(a)), thereby realizing an

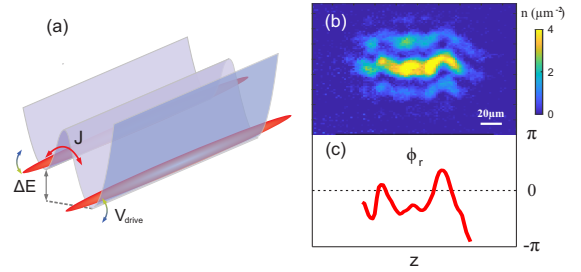


FIG. 1. (a) Two atomic clouds in a tilted double-well potential, where ΔE is the energy difference between the two minima. For $\Delta E = 0$ the barrier results in tunnel coupling J , completely suppressed for $\Delta E \gg \hbar\omega_J$ (see text). Floquet engineering is realized by periodically modulating the energy difference ΔE with an amplitude V_{drive} . (b) Typical matter-wave interference pattern after 15.6 ms Time-of-Flight with atom density depicted in color and (c) the extracted relative phase $\phi_r(z)$ between the two superfluids.

extended Josephson junction (JJ). For $\Delta E = 0$ such a system is a quantum simulator for the sine-Gordon (SG) quantum field theory [27–29]. The Josephson frequency $\omega_J = \sqrt{4J\mu/\hbar}$ is determined by the on-site interaction energy μ and the tunneling strength J in the balanced (untilted) DW. Tunneling between the two superfluids can be completely suppressed by tilting the DW with an energy difference $\Delta E \gg \hbar\omega_J$. Floquet engineering enables us to revive the tunnel coupling within the tilted DW through a periodic modulation $\Delta E(t) = \Delta E_0 + 2V_{\text{drive}} \sin(\omega t + \varphi_{\text{drive}})$.

If the modulation frequency ω is near resonant with ΔE_0 , Floquet assisted tunneling will re-couple the two superfluids, even if the amplitude $V_{\text{drive}} \ll \Delta E_0$. After time-averaging over this fast modulation, the system can effectively be treated as a static balanced DW. In the rotating Floquet frame, the time averaged Hamiltonian in the two-mode approximation is given by [29, 30]

$$\langle \tilde{H}(t) \rangle = -\hbar \tilde{J} \begin{pmatrix} 0 & e^{-i(\varphi_{\text{drive}} + \pi/2)} \\ e^{+i(\varphi_{\text{drive}} + \pi/2)} & 0 \end{pmatrix}, \quad (1)$$

where $\tilde{J} = J \times \mathcal{B}_1(\frac{2V_{\text{drive}}}{\hbar\omega})$ is the revived effective tunneling strength and \mathcal{B}_1 is the first order Bessel function. The ground state of the Hamiltonian (1) takes the form

$$|\tilde{\Psi}_{\text{ground}}\rangle = \frac{1}{\sqrt{2}} \begin{pmatrix} \exp[-i(\frac{\varphi_{\text{drive}}}{2} + \frac{\pi}{4})] \\ \exp[+i(\frac{\varphi_{\text{drive}}}{2} + \frac{\pi}{4})] \end{pmatrix}, \quad (2)$$

The amplitude and phase of the tunneling term in the Floquet Hamiltonian Eq. (1) can be controlled through the amplitude V_{drive} and phase φ_{drive} of the modulation. For the ground state Eq. (2), the latter results in a non-zero relative phase $\tilde{\phi}_r = \varphi_{\text{drive}} + \pi/2$ between the two superfluids when $\varphi_{\text{drive}} \neq -\pi/2$. Transforming the relative phase $\tilde{\phi}_r$ in the rotating Floquet frame back to the laboratory frame, the measured relative phase between the two wells is given by

$$\phi_r = \tilde{\phi}_r + \Delta E_0 t / \hbar - \frac{2V_{\text{drive}}}{\hbar\omega} \cos(\omega t + \varphi_{\text{drive}}). \quad (3)$$

Hence, when $\varphi_{\text{drive}} = -\pi/2$, the initial state with $\phi_r = 0$ in lab frame is also the ground state with $\tilde{\phi}_r = 0$ in the Floquet frame. On the other hand, for an arbitrary modulation phase φ_{drive} , the state $\phi_r = 0$ is, in the Floquet frame, mapped to a JJ with a non-vanishing starting phase $\Delta\tilde{\phi}_{r,0} = \frac{2V_{\text{drive}}}{\hbar\omega} \cos(\varphi_{\text{drive}}) - \varphi_{\text{drive}} - \pi/2$. For later convenience, we introduce $\Delta\tilde{\phi}_r = \tilde{\phi}_r - \varphi_{\text{drive}} - \pi/2$, which shifts the ground state of the JJ back to zero phase. The ability to tune the coupling strength and initial relative phase of such an extended bosonic JJ establishes the building block for more elaborate Floquet engineering.

Floquet assisted tunneling.— We first consider the simplest case, preparing the initial state as the ground state in the Floquet frame, i.e. choosing the modulation phase $\varphi_{\text{drive}} = -\pi/2$: We start in a strongly phase locked initial state with $\phi_r \approx 0$, prepared by cooling into a strongly coupled, balanced DW. We then completely suppress the tunneling between the two wells rapidly by introducing an energy difference $\Delta E_0 = h \times 411 \text{ Hz} \gg \hbar\omega_J$ and, at the same time, begin the periodic modulation $\Delta E(t)$. We choose the driving frequency $\omega = \Delta E_0 / \hbar$ resonant with the energy detuning and a driving amplitude $V_{\text{drive}} = h \times 85 \text{ Hz}$, leading to an expected revived tunneling strength of $\tilde{J} \approx 0.2J$.

In Figure 2 we present such a Floquet assisted tunneling experiment (left column) and compare it to the static tilted DW (right column). Figure 2(a) shows the time evolution for the spatially averaged relative phases (blue dots), in good agreement with the theoretical predictions (red line) given by Eq. (3) with $\tilde{\phi}_r = 0$. The insets show the full distribution functions of ϕ_r for the initial and final states. The observed broadening of the distribution reflects the relaxation in the SG model following a quench to a lower coupling \tilde{J} . The small, random deviations $\Delta\tilde{\phi}_r$ (Fig. 2(b)) represent the fluctuations of the field within the Floquet engineered SG Hamiltonian.

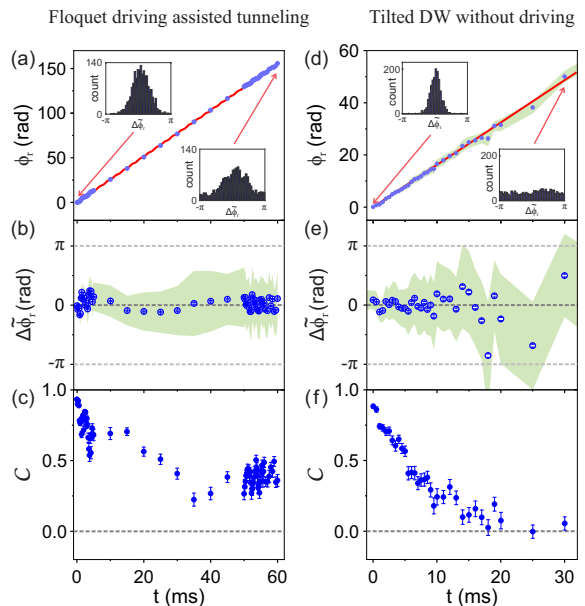


FIG. 2. (left) Floquet driven DW: $\Delta E = h \times 411 \text{ Hz}$ with Floquet drive $\omega = 2\pi \times 411 \text{ Hz}$, starting phase $\varphi_{\text{drive}} = -\pi/2$ and modulation amplitude $V_{\text{drive}} = h \times 85 \text{ Hz}$: (a) Evolution of the relative phase ϕ_r , calculated via the ensemble and spatially averaged circular mean of $\phi_r(z)$ and shifted by $2\pi N$; (b) difference $\Delta\tilde{\phi}_r$ between the measured relative phase ϕ_r and the estimate from Floquet theory; (c) Coherence factor. (right) (d-f) Comparison to a static tilted DW with $\Delta E = h \times 258 \text{ Hz}$. Blue dots: experimental data. Red line: prediction from Floquet theory. The insets in (a) and (d) show the experimental distribution of $\Delta\tilde{\phi}_r(z)$ and the light green region in (b), (d) and (e) display its standard deviation. The error bars give the standard error of the mean.

The revived tunneling strength \tilde{J} can be quantified via the coherence factor $\mathcal{C} = \langle \cos(\phi_r) \rangle$, depicted in Fig. 2(c). The initial state with $\phi_r \approx 0$ shows almost perfect phase coherence $\mathcal{C} > 0.9$, whereas for $\mathcal{C} \approx 0$ the relative phase is completely random. At early times, $t \lesssim 5 \text{ ms}$, we observe a fast decrease of coherence due to quasi-particle dephasing caused by the quench to a smaller effective tunneling coupling \tilde{J} . For $t \gtrsim 30 \text{ ms}$ the system reaches a quasi-steady state with an average coherence factor $\mathcal{C} \approx 0.38$ (Fig. 2(c)). This demonstrates that the system retains finite coherence due to a non-vanishing Floquet assisted tunneling coupling, even after relaxation.

For comparison we show in Fig. 2(d)-(f) the evolution for a static tilted DW with $\Delta E_0 = h \times 258 \text{ Hz}$ and no periodic modulation (i.e. $V_{\text{drive}} = 0$). The evolution of the relative phase within the first 10 ms is in good agreement with Eq. (3). The constant energy difference ΔE_0 only leads to a monotonic accumulation of a relative phase. For $t \gtrsim 20 \text{ ms}$ the total suppression of the initial tunneling leads to a fully random phase distribution (Fig. 2(d), inset) and consequently a vanishing coherence factor $\mathcal{C} \approx 0$. The detuning ΔE_0 was chosen to

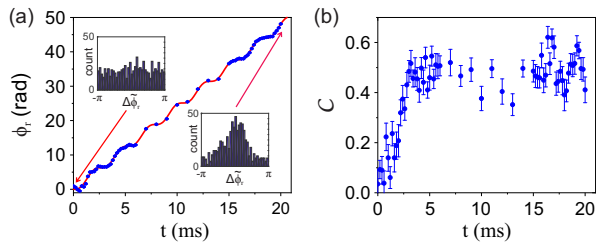


FIG. 3. The evolution of (a) relative phase ϕ_r and (b) coherence factor \mathcal{C} of two initially uncorrelated Bose gases after switching on Floquet assisted tunneling. The driving is resonant with the energy difference of the DW: $\omega = 2\pi \times 380$ Hz and its amplitude is: $V_{\text{drive}} = h \times 190$ Hz.

be the minimal energy difference between the two wells in the periodically modulated case. Consequently $\mathcal{C} \rightarrow 0$ in Fig. 2(f) verifies the complete suppression of static coupling in the Floquet system at any time and $\mathcal{C} \gg 0$ in Fig. 2(c) can only come from tunneling revived through Floquet engineering.

In the next experiment, we demonstrate that Floquet engineering can be used to recouple two independent superfluids, leading to the build up of coherence between the two wells. As before, we prepare the system in a balanced DW, but now with a high barrier and an initial coupling $J \approx 0$. Hence, the initial state after cooling is completely uncorrelated, i.e. the relative phase distribution is fully random and $\mathcal{C} \approx 0$. We subsequently lower the barrier height between the two wells while at the same time suppressing the coupling J by introducing an energy difference $\Delta E_0 = h \times 380$ Hz. The reshaping of the DW potential is done within 5 ms, short compared to the tunneling time ($\sim 2\pi/\omega_J$) but sufficiently long to avoid radial excitations ($\sim 2\pi/\omega_\perp$). Thereafter, we proceed with our usual Floquet modulation with frequency $\omega = \Delta E_0/h$ and amplitude $V_{\text{drive}} = h \times 190$ Hz which recouples the DW.

Figure 3 shows the time evolution of the relative phase ϕ_r and the coherence factor \mathcal{C} for such a Floquet recoupling experiment. The evolution of the relative phase ϕ_r shows good agreement with the theoretical predictions. The initial distribution of $\tilde{\phi}_r$ is uniform but rapidly narrows around zero (see insets), illustrating the buildup of coherence between the two wells. This is also clearly visible in the increase of the coherence factor \mathcal{C} depicted in Fig. 3(b). Within the first 5 ms, corresponding to only 2 periods of the modulation, \mathcal{C} increases to its plateau value $\mathcal{C} \approx 0.5$. This demonstrates fast phase locking by tunneling restored through Floquet engineering.

Tunneling strength and heating.— Having established Floquet engineered tunneling, we proceed to a detailed experimental analysis of the tunneling strength \tilde{J} and the long time evolution of the system. Figure 4(a-f) shows the time evolution of the coherence factor \mathcal{C} for six different driving amplitudes V_{drive}/h ranging from 0 to 155 Hz.

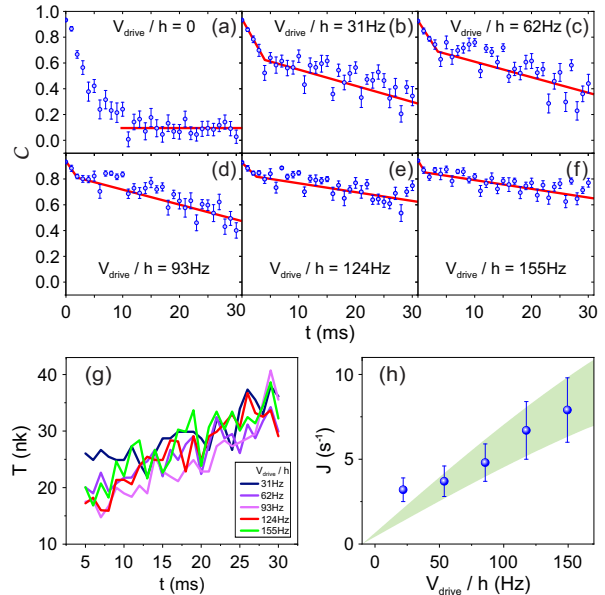


FIG. 4. (a-f). The evolution of the coherence factor \mathcal{C} under Floquet driving with different amplitudes. The red lines are linear fits highlighting the two different time regimes discussed in the text. (g) The heating rates for the driven systems in (b-f). (h) Dependence of the Floquet induced Josephson tunneling on the driving amplitude. Blue dots: experiment; light green region: estimation from Floquet theory.

The experimental sequence and all other parameters are the same as for Fig. 2(a-c). Qualitatively, the increase of the Floquet engineered coupling \tilde{J} is readily apparent from the increase of \mathcal{C} with the amplitude V_{drive} .

The time evolution shown in Fig. 4(b-f) can clearly be divided into two stages: Within the first 5 ms, the quench of the tunneling coupling from J to $\tilde{J} < J$ leads to quasi-particle dephasing and results in a rapid decline of \mathcal{C} . This is consistent with previous observations for the relaxation following a quench in static DW potentials [31–33]. In the second stage, $t \gtrsim 5$ ms, we observe a further slow decline of coherence due to heating.

We self-consistently extract the Floquet tunneling coupling \tilde{J} and the time dependent temperature (Fig. 4(g)) by comparing the measured correlation functions after dephasing to SG model predictions in thermal equilibrium [28, 34, 35] under the assumption that the Floquet tunneling strength \tilde{J} stays constant during the driving. Remarkably the derived heating rate $\Gamma \sim 0.6$ nK/ μ s is rather independent of the driving amplitude V_{drive} (see S1).

Equivalently, using the initial temperature and correlation functions we determine the initial tunneling coupling $J = 23 \pm 5$ s $^{-1}$ in the initial balanced DW. In Fig. 4(h) we compare the measured \tilde{J} to the calculated Floquet tunneling strengths Eq. (1). We find good agreement between experimental results and Floquet theory.

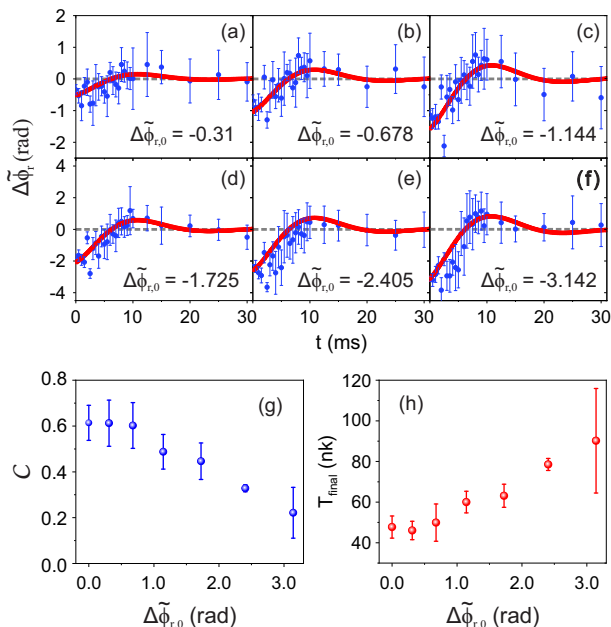


FIG. 5. (a-f) Josephson oscillations starting from different initial relative phases $\Delta\tilde{\phi}_{r,0}$ in the rotating Floquet frame. The red line is fitted with the assumption that the Josephson frequencies ω_J and the decay rates τ are independent of the initial phase $\Delta\tilde{\phi}_{r,0}$. (g) Coherence factor and (h) temperature of the system after 20 ms of driving for different initial relative phase $\Delta\tilde{\phi}_{r,0}$.

The common mode temperature of the system before and after 30 ms of Floquet driving was measured by density correlation functions after 11.2 ms ToF [26]. We found no significant heating in the common mode (see S1 and [29] for details).

Josephson oscillations and relaxation.— Finally we consider different driving phases φ_{drive} of the modulation, which imprints an initial relative phase difference $\Delta\tilde{\phi}_{r,0}$ directly in the Floquet frame. This realizes an extended JJ and permits precise control over the initial conditions. In the experiments we implement the same experimental Floquet sequence as before, starting from a strongly tunneling coupled state with $\phi_r \approx 0$ and $C \approx 0.9$, detuning $\Delta E_0 = h \times 436$ Hz, and driving amplitude $V_{\text{drive}} = h \times 93$ Hz, but now considering different driving phases $\varphi_{\text{drive}} = 0, \pm\pi/6, \pm\pi/3, \pm\pi/2$. Using Eq. (3), we get the initial phase differences $\Delta\tilde{\phi}_{r,0} \in [-\pi, 0]$.

Figure 5(a-f) shows the time evolution of the relative phase for different φ_{drive} . In all cases we find strongly damped Josephson oscillations, in accordance with previous experiments in static DW potentials [36].

We quantify the evolution by fitting a damped oscillation in order to extract the Josephson frequency ω_J and the characteristic damping time τ . From the previous section, we expect a Floquet tunneling strength $\tilde{J} \approx 4.8 s^{-1}$ and $\omega_J \approx 2\pi \times 46$ Hz, independent of

φ_{drive} . We therefore fit the experimental data with a single Josephson frequency and damping time, leading to $\omega_J^{\text{fit}} = 2\pi \times 40(3)$ Hz and $\tau^{\text{fit}} = 8.8(1.2)$ ms respectively. Note that ω_J^{fit} agrees with the theoretical expectations within the statistical error, thus being in good agreement with the exact Floquet predictions for J . The damping time τ^{fit} is compatible with damping times observed in static DW potentials [36, 37].

We consistently observe relaxation to a stationary state after $t \gtrsim 20$ ms. This indicates transfer of the initial potential energy, driving the coherent Josephson oscillation, into fluctuations of the relative phase [38]. In Fig. 5(g,h) we show the time-averaged coherence factor C and final temperature of the system for $t > 20$ ms, respectively. The decrease (increase) of coherence (temperature) with $\Delta\tilde{\phi}_{r,0}$ reflects the increased potential energy $\sim \tilde{J} \cos(\Delta\tilde{\phi}_{r,0})$ of the initial state. Notably, we again find the common mode temperatures to remain approximately constant throughout the evolution.

Conclusion.— Floquet engineering allows to revive the tunnel coupling in a tilted double well, creating an extended bosonic Josephson junction. We find excellent quantitative agreement between the experimental results and theoretical predictions. The periodic modulation technique developed in this work will greatly expand the freedom of manipulating such double well systems and open up new ways to study many intriguing fundamental phenomena with broad relevance ranging from condensed matter physics to cosmology.

We thank I. Mazets, B. Rauer and M. Serbyn for helpful discussions. This work is supported by the DFG/FWF Collaborative Research Centre ‘SFB 1225 (ISOQUANT)’, and by the Wiener Wissenschafts- und TechnologieFonds (WWTF), Project No.MA16-066 (SEQUEX). F.C., F.S.M., and J. Sabino acknowledge support by the Austrian Science Fund (FWF) in the framework of the Doctoral School on Complex Quantum Systems (CoQuS). T.S. acknowledges support from the Max Kade Foundation through a postdoctoral fellowship. S.-C.J. and S.E. acknowledges support through an ESQ (Erwin Schrödinger Center for Quantum Science and Technology) fellowship funded through the European Union’s Horizon 2020 research and innovation program under Marie Skłodowska-Curie Grant Agreement No 801110. This project reflects only the author’s view, the EU Agency is not responsible for any use that may be made of the information it contains. ESQ has received funding from the Austrian Federal Ministry of Education, Science and Research (BMBWF). J. Sabino acknowledges support by the Fundação para a Ciência e a Tecnologia (PD/BD/128641/2017).

* schmiedmayer@atomchip.org

- [1] C. Weitenberg and J. Simonet, Tailoring quantum gases by floquet engineering, *Nature Phys.* **17**, 1342 (2021).
- [2] A. Eckardt, Colloquium: Atomic quantum gases in periodically driven optical lattices, *Rev. Mod. Phys.* **89**, 011004 (2017).
- [3] N. Goldman, J. Dalibard, M. Aidelsburger, and N. R. Cooper, Periodically driven quantum matter: The case of resonant modulations, *Phys. Rev. A* **91**, 033632 (2015).
- [4] H. Lignier, C. Sias, D. Ciampini, Y. Singh, A. Zenesini, O. Morsch, and E. Arimondo, Dynamical control of matter-wave tunneling in periodic potentials, *Phys. Rev. Lett.* **99**, 220403 (2007).
- [5] E. Kierig, U. Schnorrberger, A. Schietinger, J. Tomkovic, and M. K. Oberthaler, Single-particle tunneling in strongly driven double-well potentials, *Phys. Rev. Lett.* **100**, 190405 (2008).
- [6] A. Eckardt, M. Holthaus, H. Lignier, A. Zenesini, D. Ciampini, O. Morsch, and E. Arimondo, Exploring dynamic localization with a bose-einstein condensate, *Phys. Rev. A* **79**, 013611 (2009).
- [7] M. Aidelsburger, M. Atala, M. Lohse, J. T. Barreiro, B. Paredes, and I. Bloch, Realization of the Hofstadter Hamiltonian with ultracold atoms in optical lattices, *Phys. Rev. Lett.* **111**, 185301 (2013).
- [8] H. Miyake, G. A. Siviloglou, C. J. Kennedy, W. C. Burton, and W. Ketterle, Realizing the Harper Hamiltonian with laser-assisted tunneling in optical lattices, *Phys. Rev. Lett.* **111**, 185302 (2013).
- [9] J. Dalibard, F. Gerbier, G. Juzeliūnas, and P. Öhberg, Colloquium: Artificial gauge potentials for neutral atoms, *Rev. Mod. Phys.* **83**, 1523 (2011).
- [10] J. Struck, C. Ölschläger, R. Le Targat, P. Soltan-Panahi, A. Eckardt, M. Lewenstein, P. Windpassinger, and K. Sengstock, Quantum simulation of frustrated classical magnetism in triangular optical lattices, *Science* **333**, 996 (2011).
- [11] J. Struck, C. Ölschläger, M. Weinberg, P. Hauke, J. Simonet, A. Eckardt, M. Lewenstein, K. Sengstock, and P. Windpassinger, Tunable gauge potential for neutral and spinless particles in driven optical lattices, *Phys. Rev. Lett.* **108**, 225304 (2012).
- [12] B. K. Stuhl, H.-I. Lu, L. M. Ayccock, D. Genkina, and I. B. Spielman, Visualizing edge states with an atomic Bose gas in the quantum Hall regime, *Science* **349**, 1514 (2015).
- [13] M. Mancini, G. Pagano, G. Cappellini, L. Livi, M. Rider, J. Catani, C. Sias, P. Zoller, M. Inguscio, and L. Fallani, Observation of chiral edge states with neutral fermions in synthetic Hall ribbons, *Science* **349**, 1510 (2015).
- [14] X.-J. Liu, X. Liu, C. Wu, and J. Sinova, Quantum anomalous Hall effect with cold atoms trapped in a square lattice, *Phys. Rev. A* **81**, 033622 (2010).
- [15] Z. Wu, L. Zhang, W. Sun, X.-T. Xu, B.-Z. Wang, S.-C. Ji, Y. Deng, S. Chen, X.-J. Liu, and J.-W. Pan, Realization of two-dimensional spin-orbit coupling for Bose-Einstein condensates, *Science* **354**, 83 (2016).
- [16] V. L. Pokrovsky and A. L. Talapov, Ground state, spectrum, and phase diagram of two-dimensional incommensurate crystals, *Phys. Rev. Lett.* **42**, 65 (1979).
- [17] A. Lazarides, O. Tieleman, and C. Morais Smith, Pokrovsky-Talapov model at finite temperature: A renormalization-group analysis, *Phys. Rev. B* **80**, 245418 (2009).
- [18] V. Kasper, J. Marino, S. Ji, V. Gritsev, J. Schmiedmayer, and E. Demler, Simulating a quantum commensurate-incommensurate phase transition using two Raman-coupled one-dimensional condensates, *Phys. Rev. B* **101**, 224102 (2020).
- [19] P. Bak, Commensurate phase, incommensurate phases and the devil's staircase, *Rep. Prog. Phys.* **45**, 587 (1982).
- [20] M. A. Amin, M. P. Hertzberg, D. I. Kaiser, and J. Karouby, Nonperturbative dynamics of reheating after inflation: A review, *Int. J. Mod. Phys. D* **24** (2015).
- [21] S. Coleman, Fate of the false vacuum: Semiclassical theory, *Phys. Rev. D* **15**, 2929 (1977).
- [22] R. Folman, P. Krüger, D. Cassettari, B. Hessmo, T. Maier, and J. Schmiedmayer, Controlling cold atoms using nanofabricated surfaces: Atom chips, *Phys. Rev. Lett.* **84**, 4749 (2000).
- [23] J. Reichel and V. Vuletic, *Atom Chips* (Wiley, VCH, 2011).
- [24] S. Hofferberth, I. Lesanovsky, B. Fischer, J. Verdu, and J. Schmiedmayer, Radiofrequency-dressed-state potentials for neutral atoms, *Nature Phys.* **2**, 710 (2006).
- [25] I. Lesanovsky, T. Schumm, S. Hofferberth, L. M. Andersson, P. Krüger, and J. Schmiedmayer, Adiabatic radio-frequency potentials for the coherent manipulation of matter waves, *Phys. Rev. A* **73**, 033619 (2006).
- [26] S. Manz, R. Bücker, T. Betz, C. Koller, S. Hofferberth, I. E. Mazets, A. Imambekov, E. Demler, A. Perrin, J. Schmiedmayer, and T. Schumm, Two-point density correlations of quasicondensates in free expansion, *Phys. Rev. A* **81**, 031610 (2010).
- [27] V. Gritsev, A. Polkovnikov, and E. Demler, Linear response theory for a pair of coupled one-dimensional condensates of interacting atoms, *Phys. Rev. B* **75**, 174511 (2007).
- [28] T. Schweigler, V. Kasper, S. Erne, I. Mazets, B. Rauer, F. Cataldini, T. Langen, T. Gasenzer, J. Berges, and J. Schmiedmayer, Experimental characterization of a quantum many-body system via higher-order correlations, *Nature* **545**, 323 (2017).
- [29] see supplemental material for details.
- [30] M. Grifoni and P. Hänggi, Driven quantum tunneling, *Phys. Rep.* **304**, 229 (1998).
- [31] S. Hofferberth, I. Lesanovsky, B. Fischer, T. Schumm, and J. Schmiedmayer, Non-equilibrium coherence dynamics in one-dimensional Bose gases, *Nature* **449**, 324 (2007).
- [32] M. Gring, M. Kuhnert, T. Langen, T. Kitagawa, B. Rauer, M. Schreitl, I. Mazets, D. Smith, E. Demler, and J. Schmiedmayer, Relaxation and prethermalization in an isolated quantum system, *Science* **337**, 1318 (2012).
- [33] T. Schweigler, M. Gluza, M. Tajik, S. Sotiriadis, F. Cataldini, S.-C. Ji, F. S. Møller, J. Sabino, B. Rauer, J. Eisert, and J. Schmiedmayer, Decay and recurrence of non-gaussian correlations in a quantum many-body system, *Nature Phys.* **17**, 559 (2021).
- [34] P. Grišins and I. E. Mazets, Coherence and Josephson oscillations between two tunnel-coupled one-dimensional atomic quasicondensates at finite temperature, *Phys. Rev. A* **87**, 013629 (2013).
- [35] S. Beck, I. E. Mazets, and T. Schweigler, Nonperturbative method to compute thermal correlations in one-dimensional systems, *Phys. Rev. A* **98**, 023613 (2018).
- [36] M. Pigneur, T. Berrada, M. Bonneau, T. Schumm, E. Demler, and J. Schmiedmayer, Relaxation to a phase-

- locked equilibrium state in a one-dimensional bosonic josephson junction, Phys. Rev. Lett. **120**, 173601 (2018).
- [37] J.-F. Mennemann, I. E. Mazets, M. Pigneur, H. P. Stimming, N. J. Mauser, J. Schmiedmayer, and S. Erne, Relaxation in an extended bosonic josephson junction, Phys. Rev. Research **3**, 023197 (2021).
- [38] T. Schweigler, Correlations and dynamics of tunnel-coupled one-dimensional bose gases, Ph.D. Thesis TU Wien, arXiv **1908**, 00422 (2019).

SUPPLEMENTAL MATERIAL

$V_{\text{drive}}/\hbar(\text{Hz})$	$J_{\text{exp}}(s^{-1})$	$J_{\text{Flo}}(s^{-1})$	$T_r^f(\text{nK})$	$\Gamma(\text{nK/ms})$	$T_c^f(\text{nK})$
31	3.2(0.7)	1.7(0.4)	42(3)	0.50	35(3)
62	3.7(0.9)	3.4(0.7)	32(2)	0.50	34(5)
93	4.8(1.1)	5.0(1.1)	37(3)	0.60	26(4)
124	6.7(1.7)	6.6(1.4)	32(2)	0.69	28(5)
155	7.9(1.9)	8.1(1.7)	35(3)	0.64	38(5)

TABLE S1. Results for different modulation amplitudes V_{drive} corresponding to Fig. 4. Depicted values are the experimentally measured (J_{exp}) and theoretically expected (J_{Flo} , see Eq. (S7)) tunneling coupling, the heating rate (Γ), and the final temperature for both the relative (T_r^f) and common (T_c^f) degrees of freedom.

Floquet Hamiltonian engineering of DW system

The derivation of the Floquet Hamiltonian for our DW system is based on the single-particle picture

$$\begin{aligned} \hat{H}(t) &= \hat{H}_0 + \hat{H}_t \\ &= \begin{pmatrix} \Delta E_0 & -\hbar J \\ -\hbar J & 0 \end{pmatrix} + V_{\text{drive}} \sin(\omega t + \varphi_{\text{drive}}) \cdot \sigma_z, \end{aligned} \quad (\text{S1})$$

where J is the tunneling strength in the balanced double well, ΔE_0 is the energy difference between the two trap bottoms, ω is the driving frequency, φ_{drive} is the starting phase of the Floquet modulation, and σ_z is the Pauli matrix.

To simplify this Hamiltonian, we perform a unitary transformation to the Floquet frame

$$\tilde{H}(t) = \hat{R}(t) \hat{H}(t) \hat{R}^\dagger(t) - i\hbar \hat{R}(t) \frac{d\hat{R}^\dagger(t)}{dt}, \quad (\text{S2})$$

with the unitary operator

$$\hat{R}(t) = \begin{pmatrix} e^{i\frac{\Delta E_0}{\hbar}t - i\mathcal{V}(t)} & 0 \\ 0 & e^{+i\mathcal{V}(t)} \end{pmatrix}. \quad (\text{S3})$$

Here we defined

$$\mathcal{V}(t) = \frac{V_{\text{drive}}}{\hbar\omega} \cos(\omega t + \varphi_{\text{drive}}) \quad (\text{S4})$$

to shorten the notation. This eliminates the diagonal term in Eq. (S1) leading to:

$$\tilde{H}(t) = -\hbar J \begin{pmatrix} 0 & e^{+i\frac{\Delta E_0}{\hbar}t - i2\mathcal{V}(t)} \\ e^{-i\frac{\Delta E_0}{\hbar}t + i2\mathcal{V}(t)} & 0 \end{pmatrix}. \quad (\text{S5})$$

Based on the Floquet theory, we can achieve the effective Hamiltonian by calculating the time-average of Eq. (S5) in one modulation period. When the driving frequency is resonant with the energy difference, i.e. $\hbar\omega = \Delta E_0$, the time-averaged Floquet Hamiltonian is given by

$$\langle \tilde{H}(t) \rangle = -\hbar \tilde{J} \begin{pmatrix} 0 & e^{-i(\varphi_{\text{drive}} + \pi/2)} \\ e^{+i(\varphi_{\text{drive}} + \pi/2)} & 0 \end{pmatrix}, \quad (\text{S6})$$

where

$$\tilde{J} = J \cdot \mathcal{B}_1\left(\frac{2V_{\text{drive}}}{\hbar\omega}\right) \quad (\text{S7})$$

is the effective tunneling strength determined by the first order Bessel function $\mathcal{B}_1(x) = \frac{1}{2\pi} \int_{-\pi}^{\pi} d\tau e^{i(x \sin \tau - \tau)}$. From Eq. (S6), the eigenstates and corresponding eigenvalue can be easily solved:

$$|\tilde{\Psi}_{\pm}\rangle = \frac{1}{\sqrt{2}} \begin{pmatrix} \exp[-i(\frac{\varphi_{\text{drive}}}{2} + \frac{\pi}{4})] \\ \pm \exp[+i(\frac{\varphi_{\text{drive}}}{2} + \frac{\pi}{4})] \end{pmatrix} \quad (\text{S8})$$

$$\varepsilon_{\pm} = \mp \hbar \tilde{J} \quad (\text{S9})$$

As discussed in the main text, the relative phase of the eigenstate in the Floquet frame depends on the driving phase φ_{drive} , which can be controlled experimentally through the RF dressing of the DW potential. The time evolution for an arbitrary state in the Floquet frame can readily be calculated from Eq. (S6). In order to compare with the results measured in the experiment, we calculate the relative phase evolution of $|\tilde{\Psi}_+\rangle$ (red line in Fig. 2(a) and in Fig. 3(a)) and afterwards transform $\tilde{\phi}_r$ from the Floquet frame back to the laboratory frame via Eq. (3).

Sine-Gordon model for tunnel-coupled superfluids

For a static, balanced DW potential the sine-Gordon model was proposed [27] and in thermal equilibrium experimentally verified [28] to be the low energy effective description of a pair of tunneling coupled quasicondensates. A complete derivation of the Floquet engineered interacting many-body system would go far beyond the current paper. For the sake of completeness we give here a brief derivation for our static DW system, assumed to describe the time-independent Floquet Hamiltonian.

For the temperatures and atom numbers considered, both condensates, located in the left and right minimum of the DW potential, fulfill the 1D condition $\mu, k_B T \ll \hbar\omega_{\perp}$. Since dynamics along the radial directions are frozen out, we can proceed with the common dimensional reduction by integrating over the tightly confined radial directions. Tunneling through the DW barrier couples the two quantum wires, leading to the effective one-

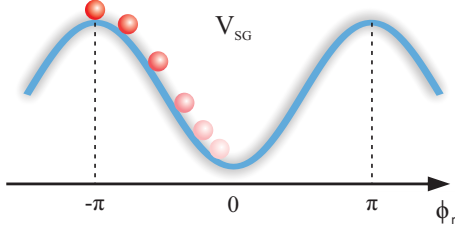


FIG. S1. Schematic of the potential energy for the sine-Gordon Hamiltonian (S12). The red spheres show the initial states for the different Floquet driving phases in Fig. 5(a)-(f). Note, that ϕ_r here corresponds to the shifted relative phase $\Delta\tilde{\phi}_r$, defined in the main text.

dimensional Hamiltonian

$$H = \sum_{j=1}^2 \int dz \left[\frac{\hbar^2}{2m} \frac{\partial \psi_j^\dagger}{\partial z} \frac{\partial \psi_j}{\partial z} + \frac{g_{1D}}{2} \partial \psi_j^\dagger \partial \psi_j^\dagger \partial \psi_j \partial \psi_j + U(z) \psi_j^\dagger \psi_j \right] - \hbar J \int dz \left[\psi_1^\dagger \psi_2 + \psi_2^\dagger \psi_1 \right]. \quad (\text{S10})$$

Here m is the atomic mass, $g_{1D} = 2\hbar a_s \omega_\perp$ is the 1D effective interaction strength, a_s is the s-wave scattering length, U is the longitudinal potential, and $2\hbar J$ is the single particle tunneling-coupling energy. The field operators fulfill the bosonic commutation relation $[\psi_j(z), \psi_{j'}^\dagger(z')] = \delta_{jj'} \delta(z - z')$.

Expressing the wave function in terms of density and phase fluctuations

$$\psi_j(z) = \exp[i\theta_j(z)] \sqrt{n_{1D} + \delta\rho_j(z)}, \quad (\text{S11})$$

with canonical commutators $[\delta\rho_j(z), \theta_{j'}(z')] = i\delta_{jj'} \delta(z - z')$,

the low-energy effective theory can be derived by expanding the Hamiltonian (S10) to second order in the small density perturbations $\delta\rho_j$ and phase gradients $\partial_z \theta_j$. This separates the Hamiltonian (S10) in a weakly coupled sum $H = H_s + H_r + V_{c,r}$ for the common (symmetric, 's') and relative (anti-symmetric, 'r') degrees of freedom (DoF), defined as

$$\begin{aligned} \delta\rho_s(z) &= \delta\rho_1(z) + \delta\rho_2(z), \quad \phi_s(z) = \frac{1}{2}[\theta_1(z) + \theta_2(z)], \\ \delta\rho_r(z) &= \frac{1}{2}[\delta\rho_1(z) - \delta\rho_2(z)], \quad \phi_r(z) = \theta_1(z) - \theta_2(z). \end{aligned}$$

Experiments in static DW potentials showed that in thermal equilibrium the coupling $V_{c,r}$ is negligible for a wide range of parameters [28], such that the common and relative DoF are described by the Luttinger-Liquid and sine-Gordon Hamiltonian, respectively. The latter is given by

$$H_r = \int dz \left[g\delta\rho_r^2 + \frac{\hbar^2 n_{1D}}{4m} (\partial_z \phi_r)^2 - 2\hbar J n_{1D} \cos(\phi_r) \right], \quad (\text{S12})$$

where, for simplicity, we consider the long wavelength limit (i.e. neglecting derivatives of the density fluctuations). The first two terms represent the Luttinger-Liquid Hamiltonian describing massless phononic excitations. A schematic of the SG potential is depicted in Fig. S1, including the initial states considered in Fig. 5(a)-(f). Their initial potential energy is transferred to fluctuations of the SG field, leading to the relaxation of the coherent Josephson oscillation in this extended bosonic JJ.